American Journal of Pathology, Vol. 159, No. 2, August 2001

Blockade of Receptor for Advanced Glycation End-Products Restores Effective Wound Healing in Diabetic Mice

Mouza T. Goova,* Jun Li,* Thomas Kislinger,* Wu Qu,* Yan Lu,* Loredana G. Bucciarelli,* Sarah Nowygrod,* Bonnie M. Wolf,† Xzabia Caliste,* Shi Fang Yan,* David M. Stern,*‡ and Ann Marie Schmidt*†

From the Departments of Surgery, Medicine,† and Physiology and Cellular Biophysics,‡ College of Physicians & Surgeons, Columbia University, New York, New York*

Receptor for advanced glycation end-products (RAGE), and two of its ligands, AGE and EN-RAGEs (members of the S100/calgranulin family of pro-inflammatory cytokines), display enhanced expression in slowly resolving full-thickness excisional wounds developed in genetically diabetic db+/db+ mice. We tested the concept that blockade of RAGE, using soluble(s) RAGE, the extracellular ligand-binding domain of the receptor, would enhance wound closure in these animals. Administration of sRAGE accelerated the development of appropriately limited inflammatory cell infiltration and activation in wound foci. In parallel with accelerated wound closure at later times, blockade of RAGE suppressed levels of cytokines; tumor necrosis factor-α; interleukin-6; and matrix metalloproteinases-2, -3, and -9. In addition, generation of thick, well-vascularized granulation tissue was enhanced, in parallel with increased levels of platelet-derived growth factor-B and vascular endothelial growth factor. These findings identify a central role for RAGE in disordered wound healing associated with diabetes, and suggest that blockade of this receptor might represent a targeted strategy to restore effective wound repair in this disorder. ***(Am J Pathol 2001, 159:513–525)***

Diabetes is associated with impaired wound healing. A number of factors have been implicated in the predisposition to nonhealing, slowly resolving, wounds observed in this disorder, such as peripheral neuropathy; altered red blood cell rheology, at least in part because of glycation of cell membrane components; glycosylation of hemoglobin and subsequent altered tissue delivery of oxygen; impaired innate host response and immune mechanisms; and peripheral microvascular disease. Irrespective of the specific etiological factor, however, it is established that effective reparative responses are impaired in diabetes leading to the development of chronic, nonhealing wounds.[1–3]

The phases of wound healing, consisting of inflammation, proliferation, and maturation/remodeling, represent a dynamic series of events that result in transformation of an open wound, into newly formed, well-vascularized granulation tissue with overlying skin enriched in collagen and other structural elements of the extracellular matrix.[4,5] In diabetes, however, abundant evidence exists that the phases of wound healing are disordered. In homeostasis, an early inflammatory phase augurs egress of neutrophils and mononuclear phagocytes from the intravascular space. These inflammatory effector cells, once released into the wounded tissue, engulf invading bacteria and promote removal of necrotic foci. In diabetes, however, decreased chemotaxis of inflammatory cells into the wound, compounded by decreased phagocytosis and intracellular killing, leads to diminished availability of factors critical for effective wound repair.[2,6–8]

These observations, together with those suggesting that diabetic wound healing is associated with diminished formation of granulation tissue and collagen, led to the premise that impaired wound healing resulted from inadequate levels of inflammatory cell-derived growth factors, such as platelet-derived growth factor (PDGF) and basic fibroblast growth factor.[9–13] A view has emerged, however, that although influx of inflammatory cells into wounded tissue is inadequate in the initial period after wounding, once established, potent inflammatory forces unique to the diabetic environment arise that sustain the generation of pro-inflammatory cytokines such as tumor necrosis factor (TNF)-α, and the production of tissue destructive matrix metalloproteinases

Supported by grants from the Surgical Research Fund, Department of Surgery, College of Physicians and Surgeons, Columbia University; the United States Public Health Service grant HL60901 (to A. M. S., S. F. Y., and D. M. S.); grant JDRF4-200-945 from the Juvenile Diabetes Research Foundation International (to A. M. S. and D. M. S.); and BWC APP 2601 from the Burroughs Wellcome Fund. L. B. is a Postdoctoral Research Fellow of the Juvenile Diabetes Research Foundation International (grant JDRF 3-2000-112), and A. M. S. is a recipient of a Burroughs Wellcome Fund Clinical Scientist Award in Translational Research.

Accepted for publication April 13, 2001.

Address reprint requests to Dr. Ann Marie Schmidt, Department of Surgery, College of Physicians & Surgeons, Columbia University, 630 W. 168th St., P&S 17-501, New York, NY 10032. E-mail: ams11@columbia.edu.

(MMPs), thereby sharply limiting effective wound closure.[14–17]

It was in this context that we speculated a role for receptor for advanced glycation end-products (RAGE) in the pathogenesis of impaired wound healing in diabetes. RAGE, a multiligand member of the immunoglobulin superfamily of cell surface molecules,[18,19] displays enhanced expression in diabetic tissues, such as blood vessels, atherosclerotic lesions, infected periodontal tissue, and glomeruli.[20–23] Two of the classes of RAGE's ligands, advanced glycation end-products (AGEs), in particular, carboxy(methyl) lysine (CML) adducts of proteins/lipids, and EN-RAGEs, members of the S100/calgranulin family of pro-inflammatory cytokines, modulate pro-inflammatory responses in a receptor-dependent manner.[18,24,25] Specifically, on endothelial cells, ligand-RAGE interaction results in induction of the procoagulant initiator tissue factor; enhanced monolayer permeability; and expression of adhesion molecules, such as VCAM-1, and cytokines, such as interleukin (IL)-6.[24–28] On mononuclear phagocytes (MPs), ligation of RAGE by AGEs or EN-RAGEs modulates chemotaxis and haptotaxis of these RAGE-bearing cells, and increases generation of cytokines, such as TNF-α, IL-6, and IL-1.[24,25,29,30] In addition, engagement of RAGE on fibroblasts results in diminished generation of collagen.[31]

Taken together, these considerations led us to hypothesize that the inevitable accumulation of AGEs within diabetic skin[32–34] provides a means, via RAGE, to transiently trap MPs and other inflammatory cells, thereby delaying their entry into wound foci. Once these cells gain access to the wound, however, we hypothesize that RAGE-bearing inflammatory cells, endothelia, and fibroblasts engage AGEs and EN-RAGES, thereby setting in motion a cascade of events eventuating in sustained influx, activation, and delayed egress of inflammatory effector cells from the wound. We speculate that enhanced interaction of RAGE with its pro-inflammatory ligands within the diabetic milieu provides a mechanism for sustained generation of cytokines and tissue-degradative MMPs, and diminished accumulation of collagen. In the present study, we tested the concept that blockade of RAGE in a model of impaired wound healing in genetically diabetic, db+/db+ mice might limit exaggerated pro-inflammatory responses, thereby abetting effective repair and wound closure.

Materials and Methods

Animals and Creation of Wounds

Genetically diabetic, male C57BLKS/J-*m*+/+*Lepr*^{db} mice (stock number 000642; Jackson Laboratories, Bar Harbor, ME) were used. Animals were maintained in a conventional animal facility with a 12-hour light/dark cycle. Water and standard rodent laboratory chow were provided *ad libitum*. At the age of 10 weeks, mice were placed in individual cages and subjected to wounding. After induction of deep anesthesia by intraperitoneal injection of ketamine (100 mg/kg; Fort Dodge, Fort Dodge, IA) and xylazine (10 mg/kg; Bayer Corporation, Shawnee Mission, KS), the hair on the surface of the mouse's back was shaved and the skin was washed with povidone-iodine solution and alcohol. A sterilized template (1.5 cm $\times$ 1.5 cm) was placed on the midback and a full-thickness excisional wound was created by removal of the skin and panniculus carnosus. Tincture of benzoin compound (Professional Disposables, Orangeburg, NJ) was applied outside the perimeter of the wound. A semipermeable transparent dressing (Tegaderm; 3M Health Care, St. Paul, MN) was placed over the wound and sealed at the edges by benzoin. On completion of the surgical procedure, animals were injected with 1 ml of NaCl (0.9%) by intraperitoneal route. Beginning on day 3 after wounding through day 10, diabetic mice were treated with murine soluble (s) RAGE. Murine sRAGE was prepared, purified, characterized, and rendered devoid of detectable endotoxin as previously described.[20] Control animals received equal amounts of vehicle, murine serum albumin (MSA) (Sigma, St. Louis, MO). Murine sRAGE or MSA was applied in sterile, endotoxin-free, phosphate-buffered saline (PBS), directly under the Tegaderm dressing; total volume, 0.1 ml/dose. In other experiments, sRAGE or MSA was administered by intraperitoneal route (50 μg/day) beginning on day 3 through 10 after wounding. After induction of deep anesthesia, blood was withdrawn from the inferior vena cava on the day of sacrifice. Levels of glycosylated hemoglobin from red blood cell lysates were determined using a kit from EG&G, Wallac, Inc. (Akron, OH). All procedures were conducted in accordance with the policies of the Institutional Animal Care and Use Committee of Columbia University.

Serial Analysis of Wound Closure

On the indicated days of, and, after wounding, the edge of the wound was traced onto a glass microscope slide. A tracing was made immediately after creation of each wound to serve as the reference point for the original area. Wound area was determined by planimetry using NIH Image 1.60 software, and reported as percent closed as calculated by the following formula: percent closure = {(area on day 0 − open area)/area on day 0} $\times$ 100. Wounds were considered closed if moist granulation tissue was no longer apparent, and the wound appeared covered with new epithelium. In all cases, to exclude pathological bacterial contamination, immediately before sacrifice, wound fluid was plated onto MacConkey II (gram-negative bacteria) and mannitol salt (gram-positive bacteria) agar plates (Becton-Dickinson and Co., Cockeysville, MD). Animals were excluded from study if any bacterial growth on these plates was observed. In our experiments, $<$5% of the animals were excluded from analysis because of bacterial contamination of the wound.

Tissue Collection and Preparation

At the time of sacrifice, immediately after final tracing of the wound edges, the entire wound, including a margin of

~5 mm of unwounded skin, was excised down to the fascia. Tissue was immediately frozen and stored at −80°C. In other cases, tissue was placed in buffered paraformaldehyde (4%) for fixation.

Preparation of Lysates for Immunoblotting and Zymography

Lysates were prepared from wound tissue by homogenization in Tris-buffered saline (Tris, 0.02 mol/L, pH 7.4, and NaCl, 0.150 mol/L) containing complete protease inhibitors (Boehringer Mannheim, Indianapolis, IN) using a homogenizer from Brinkmann (Westbury, NY). Lysates of wound tissue for gelatin zymography were prepared by homogenization in buffer containing Tris, 0.05 mol/L, pH 7.4; NaCl, 0.075 mol/L; and phenylmethylsulfonyl fluoride, 1 mmol/L. Protein concentrations were measured using an assay from Bio-Rad (Hercules, CA).

Immunoblotting

Protein extracts were prepared as described above and subjected to sodium dodecyl sulfate-polyacrylamide gel electrophoresis (Novex/Invitrogen, Carlsbad, CA). Equal amounts of protein were placed in each lane. After electrophoresis, contents of the gels were transferred to nitrocellulose membranes (Novex/Invitrogen). Nonspecific binding sites on the membranes were blocked by incubation with nonfat dry milk (5%) in Tris-buffered saline containing Tween 20 (0.1%) (blocking buffer) for 3 hours at room temperature. Primary antibody was incubated with each membrane for 16 hours at 4°C in blocking buffer. After incubation, membranes were washed in Tris-buffered saline containing Tween 20 (0.1%), followed by incubation with the appropriate peroxidase-labeled secondary antibody (diluted in blocking buffer) for 1 hour at room temperature. Membranes were washed in washing buffer and sites of antibody binding were identified using a chemiluminescence detection system (ECL; Amersham Pharmacia, Piscataway, NJ). Molecular weights (approximate) of the bands were identified by simultaneous electrophoresis of rainbow molecular markers (Amersham Pharmacia). Antibodies for immunoblotting included: goat anti-mouse IL-6 IgG (1 μg/ml; R&D Systems, Inc., Minneapolis, MN); goat anti-mouse TNF-α IgG (2 μg/ml; R&D Systems, Inc); rabbit anti-mouse PDGF-B IgG (0.4 μg/ml; Santa Cruz Biotechnology, Santa Cruz, CA); goat anti-mouse vascular endothelial growth factor (VEGF) IgG (2 μg/ml; R&D Systems, Inc.); rabbit anti-mouse RAGE, prepared and characterized as previously described[20] (2 μg/ml); mouse anti-human MMP-3 IgG (reacts with murine MMP-3) (0.1 μg/ml; Oncogene Research Products, Cambridge, MA); mouse anti-human MMP-9 IgG (reacts with murine MMP-9) (0.1 μg/ml; Oncogene Research Products); and rabbit anti-S100 IgG (2.5 μg/ml; Sigma). Bands were scanned into a laser densitometer and quantification was performed using ImageQuant software (Molecular Dynamics, Foster City, CA). Pixel units obtained from blots in MSA-treated mice were arbitrarily assigned a value of 1.0. Values for bands obtained from sRAGE-treated wound lysates were reported relative to the values obtained for MSA treatment.

Gelatin Zymography

Wound extracts were mixed with sodium dodecyl sulfate sample buffer (Novex/Invitrogen) and electrophoresed without boiling under nondenaturing conditions and placed onto gelatin-laden gels (Novex/Invitrogen). After electrophoresis, gels were incubated in renaturing buffer for 30 minutes with gentle agitation at room temperature, and then equilibrated in developing buffer for 30 minutes. Following these procedures gels were incubated in fresh developing buffer for 16 hours with gentle agitation at 37°C. Gels were stained with GELCODE Blue Stain reagent (Pierce, Rockford, IL). Areas of gelatinase activity on the gels were evident as clear bands against a dark blue background. Bands were scanned into a laser densitometer and quantification and reporting of results was performed as above.

Histology and Immunohistochemistry

Wound tissue was fixed in buffered paraformaldehyde (4%) for 16 hours, followed by paraffin-embedding and generation of sections (5 μm thick). Certain sections were stained with hematoxylin and eosin (H&E) or Direct Red 80 mixed with picric acid (Sigma) to yield Picrosirius red stain for collagen. In other cases, immunohistochemistry was performed using the following antibodies: goat anti-mouse IgG as above (1 μg/ml); goat anti-mouse TNF-α IgG (10 μg/ml; Santa Cruz Biotechnology); rabbit anti-mouse RAGE IgG (2 μg/ml); rabbit anti-EN-RAGE IgG, prepared and characterized as previously described[24] (2 μg/ml); affinity-purified anti-CML IgG, prepared and characterized as previously described[25] (0.37 μg/ml); and rat anti-mouse Mac-3 IgG (5 μg/ml; PharMingen, Franklin Lakes, NJ). In all cases, respective controls with the indicated species of nonimmune IgG were used. No specific immunostaining with control IgG was observed (not shown). Quantification of immunohistochemistry was performed as follows: multiple sections (at least four areas per slide, and at least 10 slides per condition) ($n = 3$ mice/condition) were selected by a blinded observer and imaged using a Zeiss microscope and an attached Sony video camera. For quantification of immunohistochemistry on day 10, sites for study were chosen at the edge of the wound, at the margin between normal and wounded skin. For quantification of immunohistochemistry on days 21 and 35, sites for study were selected at the center of the granulation tissue. For quantification of collagen content using Picrosirius red staining, sites were selected just below the epithelium to encompass the granulation tissue/healing wound observed on each slide. Images were analyzed by staining intensity on a Macintosh computer using the NIH Image program (version 1.62) by a

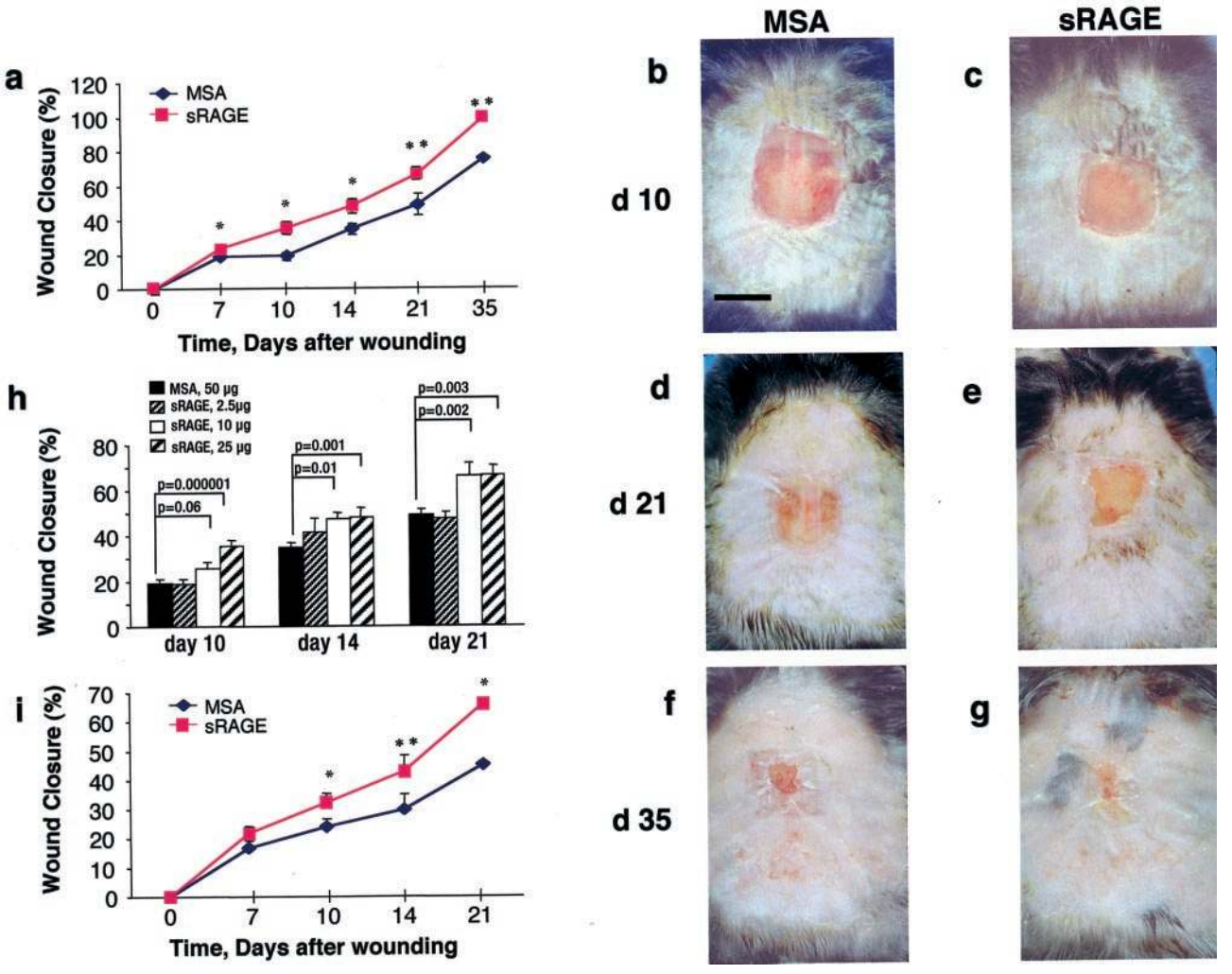

Figure 1. Administration of soluble RAGE accelerates wound healing in db+/db+ mice. Full-thickness excisional wounds (1.5 × 1.5 cm) were created on the backs of male genetically diabetic db+/db+ mice, age 10 weeks. On days 3 to 10 after wounding, murine sRAGE or serum albumin (MSA) was administered topically (**a–h**) or systemically (intraperitoneal) (**i**). Wound edges were traced onto glass microscope slides and image analysis performed to determine wound closure (%). Percent wound closure is reported as the mean ± SE. **a–g:** Time course. On days 3 through 10 after wounding, mice were treated with either MSA or sRAGE (25 μg). The following numbers of mice were used: day 7: MSA, 14; sRAGE, 17; day 10: MSA, 20; sRAGE, 17; day 14: MSA, 10; sRAGE, 17; day 21: MSA, 10: sRAGE 17; and day 35: MSA, 5; sRAGE, 4 mice. Scale bar, 1.2 cm (**b–g**). **h:** Dose response. Mice were treated with the indicated dose of sRAGE or MSA. Wounds were assessed on days 10, 14, and 21 for closure (%). The following numbers of mice were used: day 10: MSA, 20; sRAGE (2.5 μg), 12; sRAGE (10 μg), 8; sRAGE (25 μg), 17 mice; day 14: MSA, 10; sRAGE (2.5 μg), 10; sRAGE (10 μg), 10; sRAGE (25 μg), 17 mice; and day 21: MSA, 10; sRAGE (2.5 μg), 8; sRAGE (10 μg), 6; sRAGE (25 μg), 17 mice. **i:** Systemic administration of sRAGE. On days 3 to 10 after wounding, sRAGE or MSA (50 μg) was administered daily to db+/db+ mice intraperitoneally. Percent wound closure was recorded on the indicated days. The following numbers of mice were used: MSA, $n = 4$ mice; and sRAGE, $n = 7$ mice. **a** and **i:** *, $P < 0.05$; and **, indicates $P < 0.01$.

blinded observer. Specifically, on each section. a density range was set to reflect the areas stained positively with chromogen. In the case of Picrosirius red stain, bright red-staining areas were highlighted. In all cases, the number of pixels in the positive-staining sections was then divided by the total number of pixels in each field. The mean ± SE is shown for each experimental point.

Histological Score

Histological scores were determined according to previously published methods[12] by one of the investigators blinded to the experimental conditions by assessment of H&E-stained sections: 1–3, none to minimal cell accumulation and granulation tissue or epithelial travel; 4–6, thin, immature granulation dominated by inflammatory cells but with few fibroblasts, capillaries or collagen deposition and minimal epithelial migration; 7–9, moderately thick granulation tissue, ranging from being dominated by inflammatory cells to more fibroblasts and collagen deposition. This score includes extensive neovascularization; epithelium can range from minimal to moderate migration; and 10–12, thick, vascular granulation tissue dominated by fibroblasts and extensive collagen deposition. Epithelium may partially to completely cover the wound.

Statistical Analysis

Data are reported as mean ± SE. Data were analyzed by analysis of variance. Where indicated, data were subjected to post hoc comparisons using a two-tailed *t*-test.

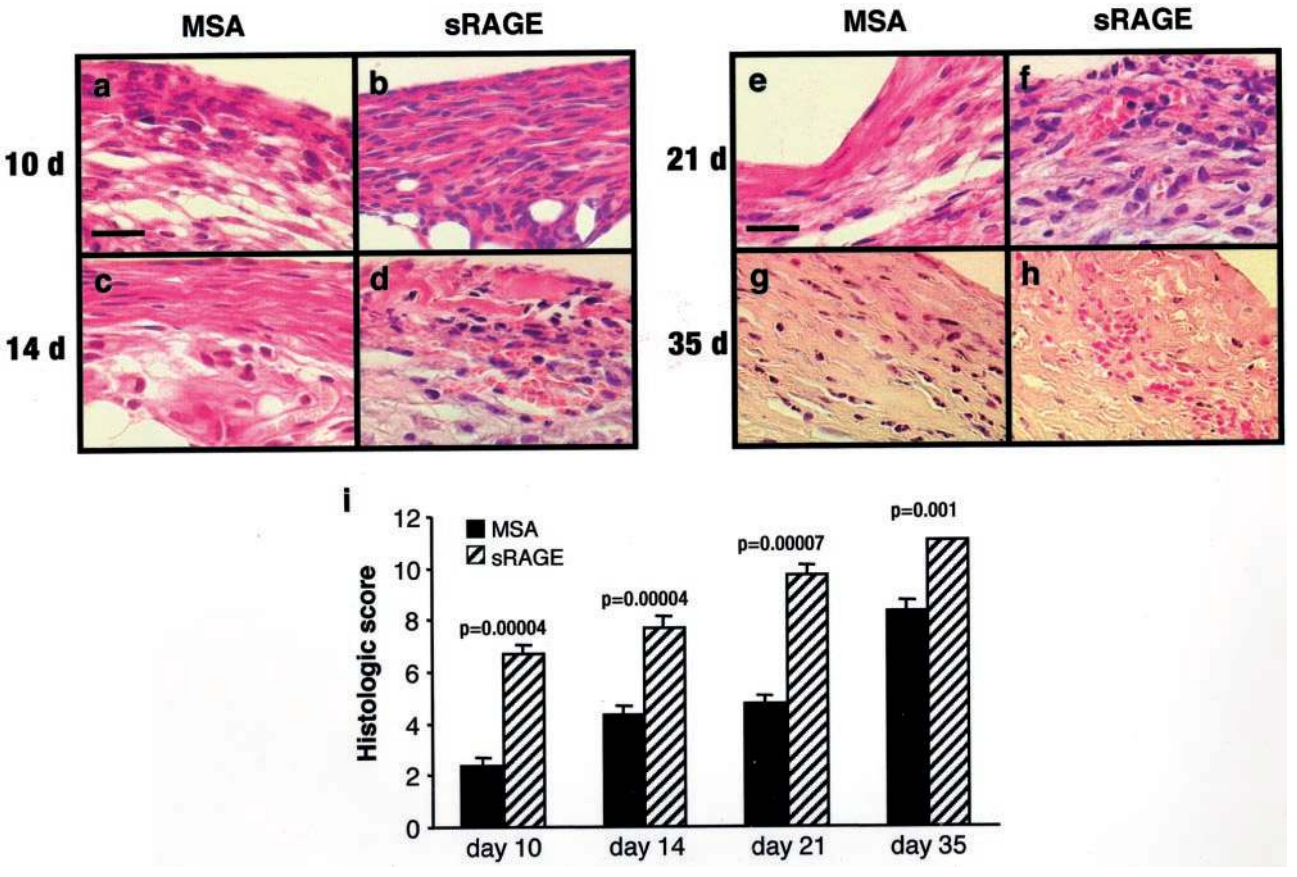

Figure 2. a–h: Administration of soluble RAGE accelerates formation of granulation tissue, re-epithelialization, and neovascularization in db+/db+ mice. Sections from wounds of db+/db+ mice treated with either sRAGE or MSA were stained with H&E and photomicrographs were prepared. On days 10 and 14, wound margins are shown, and on days 21 and 35, wound midsections are illustrated. Scale bar, 60 μm. **i:** Histological score. H&E sections from MSA- and sRAGE-treated wounds were assessed for histological score, defined as: 1–3, none to minimal cell accumulation and granulation tissue or epithelial travel; 4–6, thin, immature granulation dominated by inflammatory cells but with few fibroblasts, capillaries, or collagen deposition and minimal epithelial to 7–9, moderately thick granulation tissue, ranging from being dominated by inflammatory cells to more fibroblasts and collagen deposition. This score includes extensive neovascularization; epithelium can range from minimal to moderate migration; and to 10–12, thick, vascular granulation tissue dominated by fibroblasts and extensive collagen deposition. Epithelium may partially to completely cover the wound. On days 10, 14, 21, and 35, $n = 3$ sRAGE-treated mice per group. The following numbers of MSA-treated mice were used: day 10, 5; day 14, 6; day 21, 4; and day 35, 3.

Results

Effect of sRAGE on Wound Closure in Diabetic Mice

To test the role of RAGE in diabetic wound healing, we used the genetically diabetic db+/db+ mouse, a well-established model of insulin resistance, hyperglycemia and impaired wound healing.[12,35,36] Wound healing in these mice, primarily characterized by granulation tissue formation and re-epithelialization (≈60%), differs from that observed in nondiabetic heterozygous control (m+/db+) mice, in which wound closure ensues mostly because of contraction (≈90%).[12] To examine comparable molecular mechanisms of wound closure in the context of RAGE and its ligands, we limited our studies to db+/db+ mice. RAGE blockade in diabetic mice was achieved by administration of purified murine sRAGE, the extracellular ligand-binding domain of RAGE that binds up ligands such as AGEs and EN-RAGEs, thereby limiting engagement of cell surface receptor[20,21,24,27,37]. Control mice received vehicle (MSA). Murine sRAGE or MSA, 25 μg per day, was administered topically underneath the Tegaderm dressing from days 3 through 10 after wound creation.

Full-thickness excisional wounds were created on the backs of diabetic mice using a sterile template, 1.5 × 1.5 cm. Wound closure (percent) was assessed serially in mice treated with sRAGE or MSA. Beginning on day 7 after wounding, administration of sRAGE, 25 μg per day, accelerated processes leading to wound closure. Mice treated with sRAGE displayed 23.4 ± 1.5% closure compared with 18.5 ± 1.9% closure in MSA-treated animals ($P = 0.02$; Figure 1a). On day 10, compared to mice treated with MSA, animals treated with sRAGE displayed accelerated wound closure (19.2 ± 1.8% *versus* 35.5 ± 2.1%; $P = 0.01$) (Figure 1a). Similarly, on days 14, 21, and 35 after wounding, wound closure in sRAGE-treated mice (47.9 ± 3.6%; 66.1 ± 3.9%; and 99.1 ± 0.3%, respectively) was significantly improved compared with mice treated with MSA (34.8 ± 1.9%; 48.7 ± 2.6%; and 75.2 ± 5.9%, respectively) (Figure 1a). On days 21 and 35 after wounding, inspection of the wounds created in mice treated with MSA revealed thin, sparse granulation tissue; on day 35, wounds were not closed (Figure 1, d

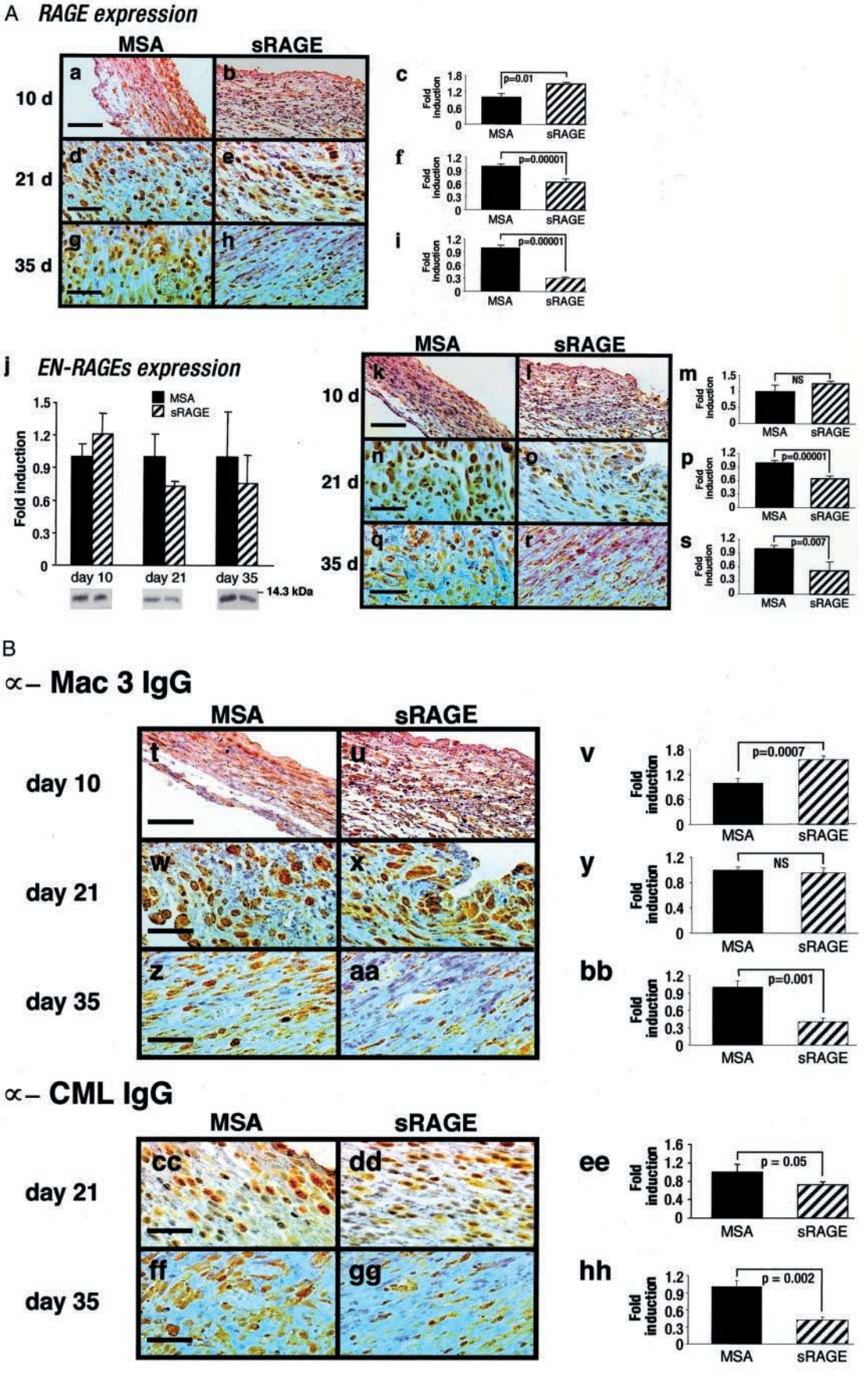
A RAGE expression
MSA
sRAGE
10 d
21 d
35 d
a
b
c
d
e
f
g
h
i
Fold induction
p=0.01
p=0.00001
p=0.00001
MSA
sRAGE
j EN-RAGEs expression
MSA
sRAGE
Fold induction
day 10
day 21
day 35
14.3 kDa
k
l
m
n
o
p
q
r
s
NS
p=0.00001
p=0.007
B
∝– Mac 3 IgG
t
u
v
w
x
y
z
aa
bb
p=0.0007
NS
p=0.001
∝– CML IgG
cc
dd
ee
ff
gg
hh
p = 0.05
p = 0.002

and f, respectively). In contrast, however, wounds in mice treated with sRAGE displayed thicker granulation tissue on days 21 and 35. By day 35, wounds were primarily healed (Figure 1, e and g).

The effects of topically applied sRAGE were dose-dependent. No significant improvement in wound closure was observed in diabetic mice treated with sRAGE, 2.5 μg per day, compared with mice receiving MSA at any time point after wounding, (Figure 1h). In contrast, mice receiving sRAGE, 10 or 25 μg per day, displayed significantly improved wound healing compared with mice treated with MSA on days 10, 14, and 21 (Figure 1h). The effects of sRAGE were not because of restoration of normoglycemia. At sacrifice, the mean level of glycosylated hemoglobin in mice treated with sRAGE, 8.1 $\pm$ 1.0%, did not differ from that observed in diabetic mice treated with MSA, 7.7 $\pm$ 0.5%. In contrast, levels of glycosylated hemoglobin in nondiabetic m+/db+ mice (n = 6) were 3.4 $\pm$ 0.2% ($P < 0.00001$ *versus* sRAGE/MSA-treated db+/db+ mice).

Importantly, systemic administration of sRAGE, 50 μg per day, by the intraperitoneal route, improved wound healing in a time-dependent manner, comparable to that achieved with topically applied soluble receptor (Figure 1i). By day 21 after wounding, sRAGE-treated db+/db+ mice displayed 65.7 $\pm$ 5.3% wound closure compared with 44.8 $\pm$ 5.0% closure observed in MSA-treated animals (P = 0.01). This observation suggests that consequent to systemic administration, sRAGE in the circulation rapidly gains access to the wound, as would be expected for a site of dramatically increased vascular permeability. In addition, we hypothesize that sRAGE in the bloodstream functions as a decoy preventing pathological activation of circulating cells, such as monocytes, that are likely to impact on reparative mechanisms operative in the wound.

Influx of Inflammatory Cells and Formation of Granulation Tissue in db+/db+ Mice: Effect of sRAGE

These observations led us to dissect the molecular mechanisms by which blockade of RAGE accelerated wound closure in diabetic mice. Analysis of H&E sections scored based on extent of inflammatory cell infiltration, neovascularization, collagen deposition, and re-epithelialization[12] provided important clues to the mechanisms underlying the effects of sRAGE. On day 10, wounds retrieved from mice treated topically with MSA displayed minimal influx of inflammatory cells at the margin between unwounded and wounded skin (Figure 2^{ii}a). In contrast, in mice treated locally with sRAGE, an extensive inflammatory cell infiltrate was noted at the wound margin on day 10 (Figure 2b). Mean histological scores on day 10 in wounds retrieved from MSA- *versus* sRAGE-treated mice indicated that sRAGE accelerated inflammatory and reparative responses within the diabetic wound (2.4 $\pm$ 0.3 *versus* 6.7 $\pm$ 0.4, respectively; P = 0.00004) (Figure 2i). On days 14 and 21, wounds retrieved from sRAGE-treated mice displayed extensive numbers of inflammatory cells, epithelial travel, and formation of new blood vessels (Figure 2, d and f). In contrast, wounds retrieved from MSA-treated mice continued to display fewer numbers of inflammatory cells and thin granulation tissue at these time points (Figure 2, c and e). On day 14, histological scores in wounds retrieved from mice receiving sRAGE or MSA were 7.7 $\pm$ 0.4 and 4.3 $\pm$ 0.4, respectively; P = 0.0004 (Figure 2i). On day 21, quantitative analysis revealed significantly diminished scores in mice treated with MSA *versus* sRAGE, 4.7 $\pm$ 0.3 *versus* 9.7 $\pm$ 0.4, respectively; P = 0.00007 (Figure 2i). By day 35, wounds retrieved from mice treated with MSA began to demonstrate increased numbers of inflammatory cells, along with new blood vessel formation and collagen deposition at the midsection. Re-epithelialization, although underway, was not nearly complete in these mice (Figure 2g). In contrast, on day 35, midsections of sRAGE-treated wounds displayed diminished numbers of inflammatory cells, extensive re-epithelialization, neovascularization, and collagen deposition (Figure 2h). Consistent with these observations, histological scores remained decreased in MSA- *versus* sRAGE-treated mice on day 35 (8.3 $\pm$ 0.4 *versus* 11.0 $\pm$ 0.0, respectively; P = 0.001) (Figure 2i). These findings supported the hypothesis that blockade of RAGE restored effective wound healing mechanisms by forging an appropriately limited period of inflammation, followed by effective proliferation and repair.

Expression of RAGE and Its Ligands in Wounds of db+/db+ Mice

Consistent with a role for RAGE in diabetic wound repair, immunohistochemistry using anti-RAGE IgG revealed fewer numbers of RAGE-bearing inflammatory cells at the wound margins on day 10 in mice treated with MSA *versus* sRAGE (Figure 3, a and b). In MSA-treated wounds, a very thin area of granulation tissue was formed. However, in sRAGE-treated wounds, an extensive layer of granulation was in place bearing increased numbers of RAGE-expressing cells (≈1.5-fold greater

Figure 3. Expression of RAGE, EN-RAGEs, Mac-3, and CML epitopes in wound tissue. **a–i:** RAGE expression. On the indicated day after wounding, wounds from MSA- and sRAGE-treated mice (topical administration) were retrieved and immunohistochemistry performed with anti-RAGE IgG. In **a** and **b**, wound margins are shown; and in **d**, **e**, **g**, and **h**, midsections are illustrated. Representative sections from at least three mice per group are shown. Quantification was performed and is reported in **c**, **f**, and **i**. **j–s:** EN-RAGE expression. **j:** Immunoblotting was performed on lysates retrieved from MSA- and sRAGE-treated wounds. Representative bands from three mice per group are shown. **k–s:** Immunochemistry. On the indicated days, MSA- and sRAGE-treated wounds were retrieved and immunostaining performed with anti-EN-RAGE IgG. In **k** and **l**, wound margins are shown and in **n**, **o**, **q**, and **r**, midsections are illustrated. Representative sections from at least three mice per group are shown. Quantification was performed and is reported in **m**, **p**, and **s**. **t–bb:** Mac-3 epitopes. **ml–hh:** CML-epitopes. On the indicated days, MSA- and sRAGE-treated wounds were retrieved and immunostaining performed with anti-Mac 3 IgG or affinity-purified anti-CML IgG. In **t** and **u**, wound margins are shown; and in **w**, **x**, **z**, **aa**, **ml**, **dd**, **ff**, **gg**, midsections are illustrated. Representative sections from at least three mice per group are shown. Quantification was performed and is reported in **v**, **y**, **bb**, **ee**, and **hh**. Scale bars: 100 μm (**a**, **b**, **k**, **l**, **t**, and **u**); 30 μm (**d**, **e**, **g**, **h**, **n**, **o**, **q**, **r**, **w**, **x**, **z**, **aa**, **ml**, **dd**, **ff**, and **gg**).

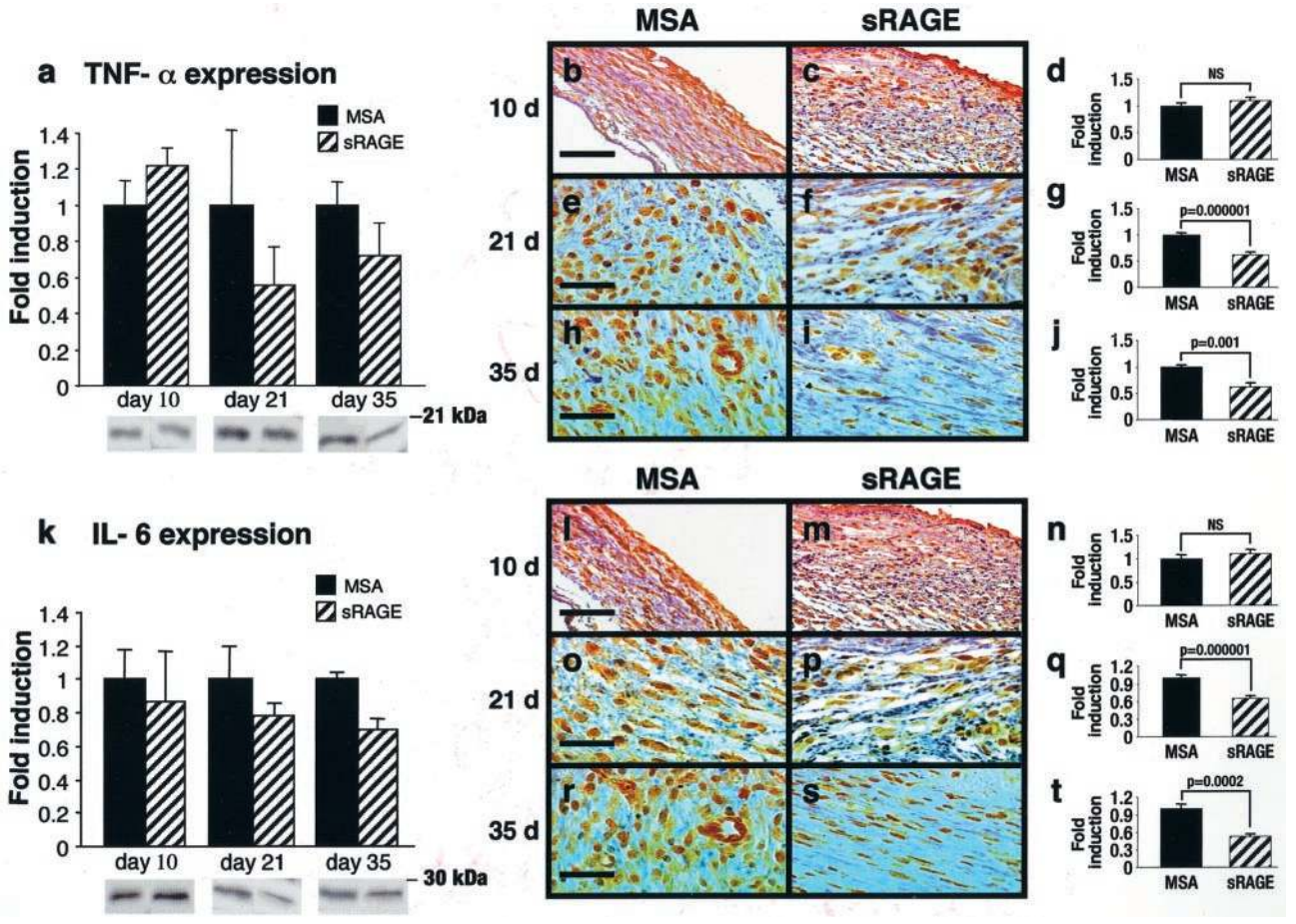

Figure 4. Expression of TNF-α and IL-6 in wound tissue. **a** and **k:** Immunoblotting was performed on lysates retrieved MSA- and sRAGE-treated wounds using anti-TNF-α IgG (**a**) or anti-IL-6 IgG (**k**). Representative bands from at least three mice per group are shown. **b–j and l–t:** Immunohistochemistry. On the indicated days, MSA- and sRAGE-treated wounds were retrieved and immunostaining performed using anti-TNF-α IgG (**b–j**) or anti-IL-6 IgG (**l–t**). In **b**, **c**, **l**, and **m** wound margins are shown; and in **e**, **f**, **h**, **i**, **o**, **p**, **r**, and **s**, midsections are illustrated. Quantification was performed and is reported in **d**, **g**, **j**, **n**, **q**, and **t**. Representative sections from at least three mice per group are shown. Scale bars: 100 μm (**b**, **c**, **l**, and **m**); 30 μm (**e**, **f**, **h**, **i**, **o**, **p**, **r**, and **s**).

than in MSA-treated wounds by quantitative immunohistochemistry; P = 0.01) (Figure 3c). On day 21 after wounding, in parallel with increased wound closure and histological evidence of repair, levels of RAGE antigen were significantly decreased in sRAGE-treated wounds compared with those receiving MSA (Figure 3, e and d, and Figure 3f; $P = 0.00001$). By day 35, consistent with ongoing cellular activation and lack of effective closure in MSA-treated wounds, numbers of RAGE-expressing cells were increased ≈3.3-fold in the presence of MSA at the midsection, compared with those treated with sRAGE (Figure 3, g and h, and Figure 3i; $P = 0.00001$). Because multiple studies have suggested that expression of RAGE is enhanced at sites of ligand deposition, we assessed levels of EN-RAGEs. EN-RAGEs, members of the family of S100/calgranulin pro-inflammatory cytokines, are expressed in a range of cell types, especially inflammatory cells, such as MPs, neutrophils, and lymphocytes.[24] Wound margins from sRAGE-treated mice on day 10 displayed increased EN-RAGE antigen by immunoblotting compared with mice treated with MSA (Figure 3j). As MPs are a principal cell type within the wound that promote the inflammatory response, we assessed levels of this key effector cell in the wound tissue. Consistent with the concept that blockade of RAGE accelerated the inflammatory response within the wound, increased numbers of MPs (≈1.6-fold), as assessed by Mac-3 antigen, were observed in margins of sRAGE-treated wounds on day 10 compared with MSA (Figure 3, u and t, and Figure 3v; $P = 0.0007$). By day 21, consistent with enhanced inflammation in vehicle-treated wounds, and decreased cellular activation in the resolving sRAGE-treated wounds, levels of EN-RAGE antigen by immunoblotting were increased in MSA-treated wounds compared with those wounds to which sRAGE had been applied (Figure 3j).

Immunohistochemical analysis revealed an ≈1.6-fold increase in EN-RAGE epitopes on day 21 in MSA- *versus* sRAGE-treated wounds (Figure 3, n and o, and Figure 3p; $P = 0.00001$). By day 35 after wounding, levels of EN-RAGE antigen by immunoblotting, were increased ≈1.3-fold in mice treated with MSA *versus* sRAGE (Figure 3j). Immunohistochemical studies confirmed these observations. On day 35, wounds from MSA-treated mice displayed an ≈1.9- and 2.5-fold increase in EN-RAGE and Mac-3 antigens in wound midsections (Figure 3, q and s, and z and bb, respectively), compared with sRAGE-treated wounds (Figure 3, r and s, and aa and bb, respectively).

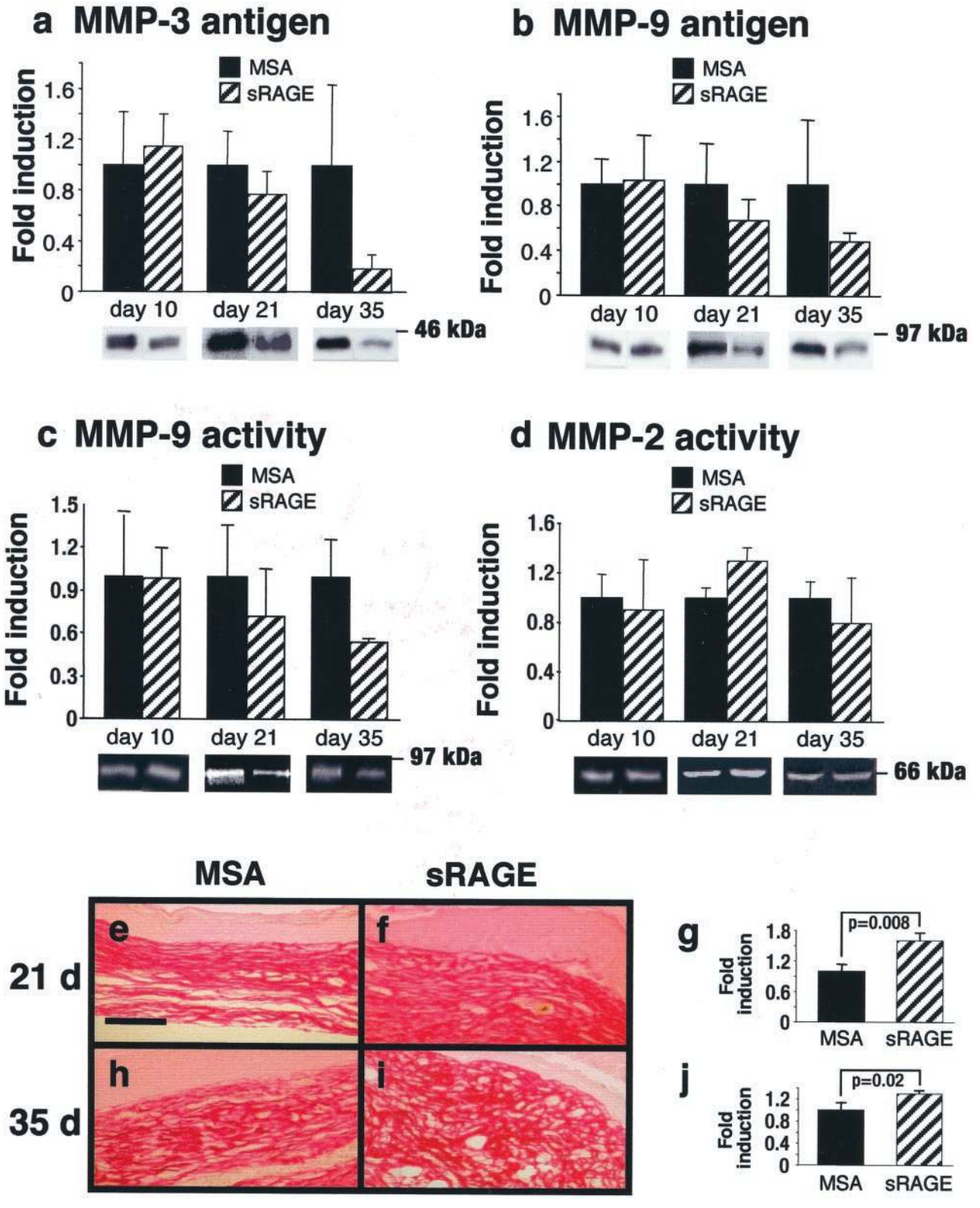

Figure 5. Expression of MMP antigen/activity, and collagen content in wound tissue. **a** and **b:** Immunoblotting was performed on lysates retrieved from MSA- and sRAGE-treated wounds using anti-MMP-3 (**a**) or anti-MMP-9 IgG (**b**). Representative bands from at least three mice per group are shown. **c–d:** Zymography was performed on lysates retrieved from MSA- and sRAGE-treated wounds. Representative bands from at three mice per group are shown. **e–j:** Picrosirius red stain. On days 21 and 35, MSA- and sRAGE-treated wounds were retrieved and sections stained with Picrosirius red. Areas of collagen in the wound midsections are indicated by red stain. Quantification was performed and is reported in **g** and **j**. Representative sections from at least three mice per group are shown. Scale bars, 100 μm (**e**, **f**, **h**, and **i**).

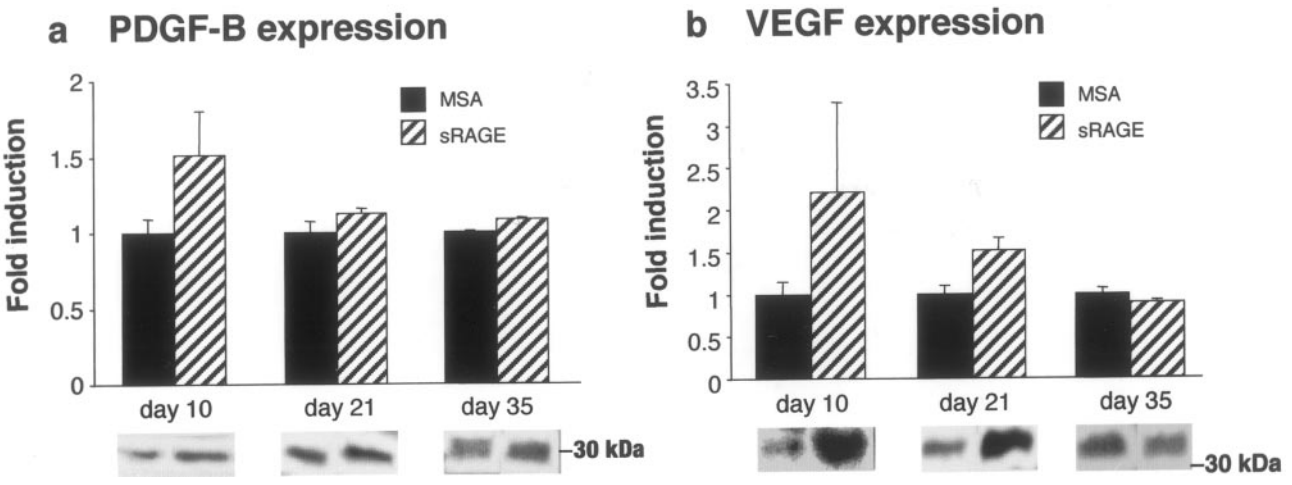

Figure 6. Expression of PDGF-B and VEGF in wound tissue. Immunoblotting was performed on lysates retrieved from sRAGE- and MSA-treated wounds using either anti-PDGF-B IgG (**a**) or anti-VEGF IgG (**b**). Representative bands from at least three to four mice per group are shown.

As studies have indicated that levels of AGE epitopes are increased in diabetic skin,[32–34] and that administration of sRAGE effects reduced levels of AGE epitopes *in vivo* in murine models,[20] we assessed levels of AGE/CML epitopes in wound tissue of db+/db+ mice by immunohistochemistry using affinity-purified anti-CML IgG.[25] On day 21 after wound creation, levels of CML epitopes in sRAGE-treated wounds were reduced ≈1.4-fold compared with wounds receiving MSA (Figure 3, dd and cc, and Figure 3ee; $P = 0.05$). By day 35, levels of CML epitopes were ≈2.5-fold greater in MSA-treated wounds, within the granulation tissue, blood vessels, and cellular elements at the wound midsection, compared with wounds treated with sRAGE (Figure 3, ff and gg, and Figure 3hh; $P = 0.002$). In sRAGE-treated wounds, newly formed epithelium, cellular elements, blood vessel structures, and collagenous deposits were primarily free of CML epitopes (Figure 3gg).

Expression of Cytokines and MMPs in Wound Tissues: Effect of sRAGE

Taken together, these observations suggested that although influx of inflammatory cells into vehicle-treated diabetic wounds was delayed, once in place, sustained cellular activation followed, leading to failure of remodeling and wound closure by day 35. Indeed, by day 21 after wounding, the tide appearing already turning in sRAGE-treated wounds, in that levels of RAGE and its ligands were already receding. To test the effects of blocking ligand-RAGE axis on levels of tissue-destructive molecules within the wound, we assessed levels of two potent pro-inflammatory cytokines. On day 10, there was no difference in expression of TNF-α in wounds treated with sRAGE or MSA (Figure 4, a–d). However, on days 21 and 35, levels of TNF-α antigen were increased ≈1.8- and 1.4-fold by immunoblotting in mice treated with MSA *versus* sRAGE, respectively (Figure 4a). Levels of TNF-α-expressing cells were increased ≈1.6-fold in MSA-treated wounds compared with those wounds receiving sRAGE on day 21 (Figure 4, e and f, and Figure 4g; $P = 0.000001$). Further, by day 35 after wounding, an ≈1.6-fold increase in levels of TNF-α was observed in MSA-*versus* sRAGE-treated wounds at the midsection (Figure 4, h and i, and Figure 4j; $P = 0.001$). Additional support for this concept was evident on assessment of levels of IL-6 in diabetic wounds. Although there was no appreciable difference in levels of IL-6 at 10 days after wounding in MSA- *versus* sRAGE-treated mice (Figure 4, k–n), on days 21 and 35, immunoblotting revealed increased expression of IL-6 antigen in MSA-treated wounds *versus* those diabetic wounds treated with sRAGE (≈1.3- and 1.4-fold, respectively) (Figure 4k). Similarly, IL-6 antigen-expressing cells in the midsections of wounds on day 21 were increased ≈1.5-fold in MSA-treated wounds *versus* those treated with sRAGE (Figure 4, o and p, and Figure 4q; $P = 0.000001$). Similarly, by day 35 after wounding, levels of IL-6 were increased ≈1.9-fold in mice treated with MSA *versus* sRAGE (Figure 4, r and s, and Figure 4t; $P = 0.0002$).

These observations suggested that once established, inflammatory responses in the diabetic wound were sustained. An important function of TNF-α in the inflammatory response is the generation of activated forms of MMPs.[38] Once activated, MMPs mediate destruction of newly formed collagen, as well as other structural matrix elements and molecules within the wound milieu. Immunoblotting studies revealed that levels of MMP-3 antigen were reduced ≈1.3-fold in sRAGE-treated *versus* MSA-treated wounds on day 21 (Figure 5a), and, by day 35, levels of MMP-3 antigen were increased ≈5.0-fold in wounds retrieved from mice treated with MSA *versus* sRAGE (Figure 5a). In addition, levels of MMP-9 antigen, nearly identical on day 10 after wounding in both groups, were elevated ≈1.5-fold and ≈2.0-fold in MSA-treated wounds *versus* those receiving sRAGE on days 21 and 35 after wound creation, respectively (Figure 5b). Analogous to these findings at the antigen level, zymography revealed an ≈1.4-fold and ≈1.9-fold increase in active MMP-9 on days 21 and 35 in MSA- *versus* sRAGE-treated wounds, respectively (Figure 5c). Furthermore, levels of MMP-2 activity were enhanced in MSA-treated wounds

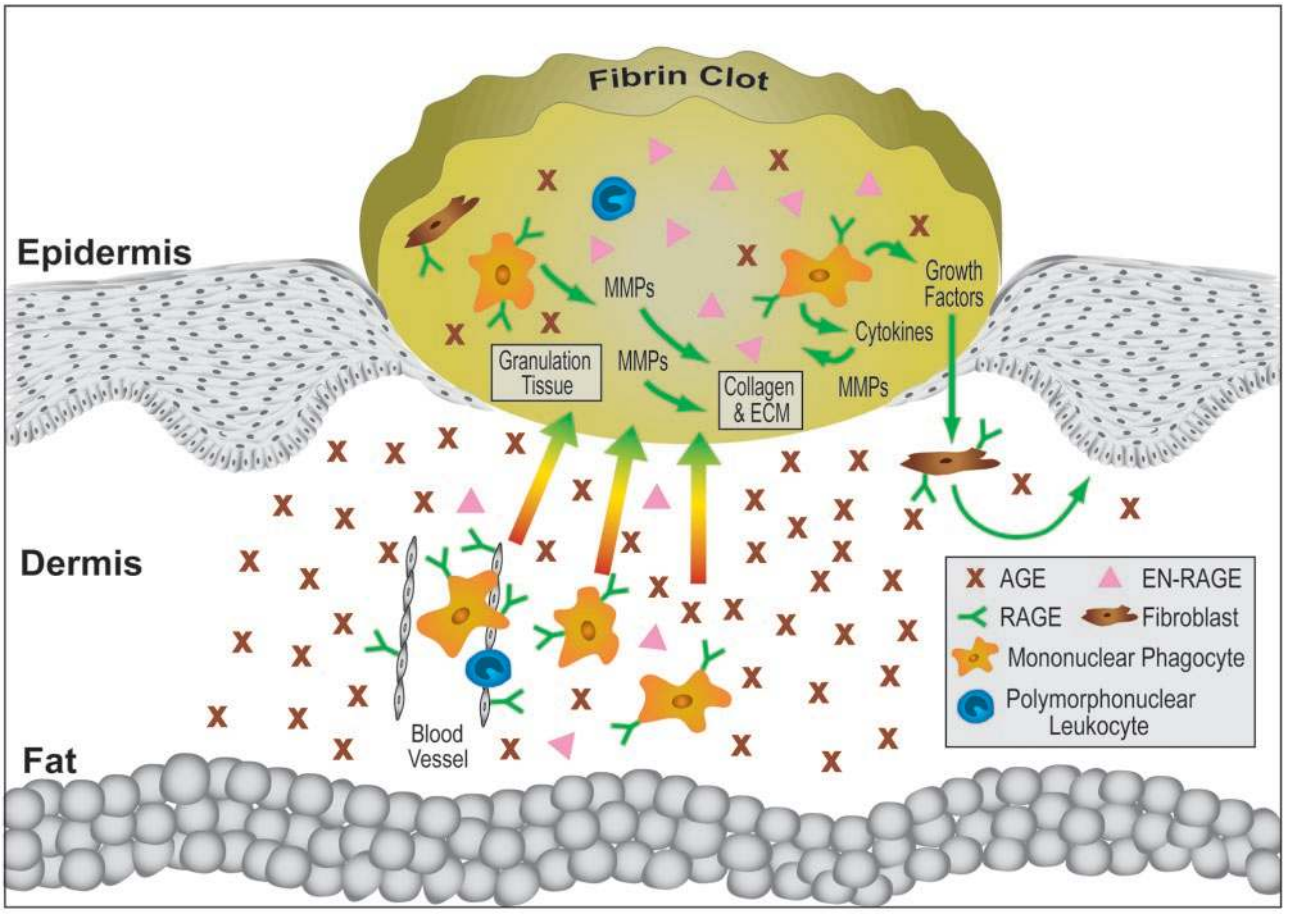

Figure 7. Blockade of RAGE restores effective wound healing in db+/db+ mice. In diabetes, influx of inflammatory cells such as PMNs and MPs into wound foci is markedly delayed. RAGE-bearing inflammatory cells are trapped by AGEs within the dermis (**arrows**; red segments). Once they gain access to the wound (**arrows**; yellow ⇒ green segments), however, inflammatory cells such as MPs, along with other RAGE-bearing effector cells (such as fibroblasts and endothelial cells), interact with AGEs and EN-RAGEs. Activation of RAGE initiates a cascade of cellular activation, typified by generation of cytokines and MMPs (**green arrows**). Delayed egress of inflammatory cells portends ongoing stimulation of RAGE, sustained inflammation, and failure of reparative/remodeling processes. We speculate that blockade of RAGE both hastens and appropriately limits the inflammatory phase of wound healing in diabetes, thereby promoting closure.

on day 35 (Figure 5d). Consistent with the concept that diminished MMP antigen and activity were evident at the later stages of wound repair in mice treated with sRAGE, Picrosirius red staining revealed significantly increased collagen in wounds treated with sRAGE compared with MSA on days 21 (Figure 5, f and e, and Figure 5g; $P = 0.008$) and 35 (Figure 5, i and h, and Figure 5j; $P = 0.02$).

Expression of PDGF-B and VEGF in Diabetic Wounds: Effect of sRAGE

An essential role of inflammatory cells infiltrating wounded skin is to promote generation of growth factors. These factors, critical for a wide array of functions designed to limit inflammation, enhance neovascularization, and modulate the laying down of new collagen, are diminished in diabetic wounds, at least in part, because of diminished influx of inflammatory effector cells in the first days after wounding.[12] Consistent with the premise that blockade of RAGE accelerated beneficial inflammatory responses in diabetic wounds, immunoblotting of lysates prepared from sRAGE-treated wounds on day 10 revealed an ≈1.5-fold increase in PDGF-B epitopes compared with wounds treated with MSA (Figure 6a). In addition, epitopes for VEGF in lysates prepared from sRAGE-treated wounds on days 10 and 21 were enhanced ≈2.2-fold, and ≈1.5-fold, respectively, by immunoblotting, compared with wounds treated with MSA (Figure 6b).

Discussion

Recent observations from clinical and experimental models of diabetes underscore the concept that sustained inflammation underlies, in large part, the failure of diabetic wounds to heal. For example, although acute human wounds in the euglycemic milieu were found to be virtually devoid of MMPs, fluids retrieved from diabetic nonhealing wounds displayed very high levels of MMPs.[39] In db+/db+ mice subjected to full-thickness excisional wounds, enhanced activity of MMP-2 and MMP-9 were observed on day 25 after wounding compared with nondiabetic controls.[40] In other studies, high levels of TNF-α and proteases in the wound were identified as key biochemical/molecular factors predictive of

failure of closure in human wounds.[41] In addition to exaggerated generation of pro-inflammatory factors, recent observations suggested that blunted apoptosis of inflammatory cells within the wound contributes to, *en balance,* sustained pro-inflammatory forces within the diabetic wound.[42,43]

It is thus not surprising that recent strategies aimed at introducing pharmacological levels of growth factors such as PDGF-BB and basic fibroblast growth factor into diabetic wounds have been met with equivocal success.[44–46] In this context, the molecular targets of MMPs are myriad, and include not only elements of the extracellular matrix, but also growth factors and other polypeptides within the wound milieu. Thus, the observation that human and murine diabetic chronic wounds are enriched in MMPs provides support for the premise that impaired growth factor availability may limit effectiveness of this strategy. Further, the observation that chronic diabetic wounds are best characterized by a sustained inflammatory response[14–17] suggests that exogenous application of single or combinations of growth factors may not address the fundamental impairment in the diabetes.

Taken together, these considerations underscore the concept that in wound healing, a fine balance must be struck between appropriately limited inflammatory responses, and those that, when sustained, portend ongoing tissue degradation. Our findings place RAGE at the center of a cascade of events that disturbs the equilibrium between beneficial and injurious inflammation in the diabetic wound. We speculate that chronic accumulation of AGEs within the skin and subcutaneous elements serves as a temporary glue, delaying the entry of blood- and tissue-derived inflammatory cells such as MPs into the wound site. Once in the wound, however, RAGE-bearing MPs and other cellular effector cells, such as lymphocytes, endothelial cells, and fibroblasts, interact with AGEs and EN-RAGEs (the latter released from invading inflammatory cells) in a sustained manner. These events prime a spiraling cascade of cellular activation, and a vicious cycle of cytokine and MMP generation, mediated, at least in part, by delayed egress of activated inflammatory cells from the wound milieu (Figure 7). Blockade of RAGE restores physiological migration of inflammatory cells into, and then out of, inflamed foci, as well as their limited activation, thereby re-setting molecular cues within the wound leading to effective inflammation and wound repair. Indeed, on day 10 after wounding, administration of sRAGE accelerated the inflammatory response, as indicated by increased levels of RAGE and EN-RAGEs, macrophages, and pro-inflammatory mediators compared with vehicle-treated wounds. However, by days 21 and 35, in parallel with increasing wound closure and histological evidence of thick granulation tissue and re-epithelialization, levels of RAGE, its ligands, macrophages, and pro-inflammatory/tissue-degradative molecules were reduced in wounds treated with sRAGE compared with those to which MSA had been applied.

These findings highlight the premise that in contrast to therapeutic strategies interfering with distinct distal effector pathways, such as specific growth factors, blockade of RAGE exerts a more proximal and global effect on the biology of the diabetic wound, affecting expression/activation of growth factors, cytokines, and MMPs. Taken together, RAGE blockade re-sets the balance between effective and deleterious inflammation, thereby promoting wound closure.

Acknowledgments

We thank Drs. Gabriel Godman and Giuseppe Andres for their advice, suggestions, and expertise.

References

1. Goodson WH, Hunt TK: Wound healing and the diabetic patient. Surg Gynecol Obstet 1979, 149:690–698
2. Morain WD, Colen LB: Wound healing in diabetes mellitus. Clin Plast Surg 1990, 17:493–501
3. Goodson WH, Hunt TK: Studies of wound healing in experimental diabetes. J Surg Res 1977, 22:221–227
4. Schaffer CJ, Nanney LB: Cell biology of wound healing. Int Rev Cytol 1996, 169:151–181
5. Ehrlich HP: The physiology of wound healing. A summary of normal and abnormal wound healing processes. Adv Wound Care 1998, 11:326–328
6. Balch HH, Watters M: Blood bactericidal studies and serum complement in diabetic patients. J Surg Res 1963, 3:199–206
7. Robson MC, Heggers JP: Effects of hyperglycemia on survival of bacteria. Surg Forum 1969, 20:56–57
8. Brayton RG, Stokes PE, Schwartz MS, Louria DB: Effect of alcohol and various diseases on leukocyte mobilization, phagocytosis and intracellular bacterial killing. N Engl J Med 1970, 282:123–128
9. Goodson W, Hunt T: Wound collagen accumulation in obese hyperglycemic mice. Diabetes 1986, 35:491–495
10. Bowersox JC: In vivo collagen metabolism in spontaneously diabetic (db/db) mice. Exp Mol Pathol 1986, 45:221–226
11. Caenazzo A, Pietrogrande F, Polato G, Piva E, Sartori D, Girolami A: Decreased platelet mitogenic activity in patients with diabetes mellitus. Hematologia 1991, 24:241–247
12. Greenhalgh D, Sprugel K, Murray M, Ross R: PDGF and FGF stimulate wound healing in the genetically diabetic mouse. Am J Pathol 1990, 136:1235–1246
13. Yue DK, Swanson B, McLennan S, Marsh M, Spaliviero J, Delbridge L, Reeve T, Turtle JR: Abnormalities of granulation tissue and collagen formation in experimental diabetes, uremia, and malnutrition. Diabet Med 1986, 3:221–225
14. Hennessey PJ, Ford EG, Black CT, Andrassy RJ: Wound collagenase activity correlates directly with collagen glycosylation in diabetic rats. J Pediatr Surg 1990, 25:75–78
15. Trengove NJ, Bielefeldt-Ohmann H, Stacey MC: Mitogenic activity and cytokine levels in non-healing and healing chronic leg ulcers. Wound Rep Reg 2000, 8:13–25
16. Inoue N, Nishikata S, Furuya E, Takita H, Kawamura M, Nishikaze O: Streptozotocin diabetes: prolonged inflammatory response with delay in granuloma formation. Int J Tissue React 1985, 7:27–33
17. Wetzler C, Kämpfer H, Stallmeyer B, Pfeilschifter J, Frank S: Large and sustained induction of chemokines during impaired wound healing in diabetic mouse: prolonged persistence of neutrophils and macrophages during the late phase of repair. J Invest Dermatol 2000, 115:245–253
18. Schmidt AM, Vianna M, Gerlach M, Brett J, Ryan J, Kao J, Esposito C, Hegarty H, Hurley W, Clauss M, Wang F, Pan YC, Tsang TC, Stern D: Isolation and characterization of binding proteins for advanced glycosylation endproducts from lung tissue which are present on the endothelial cell surface. J Biol Chem 1992, 267:14987–14997
19. Neeper M, Schmidt AM, Brett J, Yan SD, Wang F, Pan YC, Elliston K, Stern D, Shaw A: Cloning and expression of RAGE: a cell surface receptor for advanced glycosylation end products of proteins. J Biol Chem 1992, 267:14998–15004

20. Park L, Raman KG, Lee KJ, Yan L, Ferran LJ, Chow WS, Stern D, Schmidt AM: Suppression of accelerated diabetic atherosclerosis by soluble Receptor for AGE (sRAGE). Nat Med 1998, 4:1025–1031
21. Lalla E, Lamster IB, Feit M, Huang L. Spessot A, Qu W, Kislinger T, Lu Y, Stern DM, Schmidt AM: Blockade of RAGE suppresses periodontitis-associated alveolar bone loss in diabetic mice. J Clin Invest 2000, 105:1117–1124
22. Schmidt AM, Yan SD, Stern D: The dark side of glucose (news and views). Nat Med 1995, 1:1002–1004
23. Tanji N, Markowitz GS, Fu C, Kislinger T, Taguchi A, Pischetsrieder M, Stern D, Schmidt AM, D'Agati VD: The expression of advanced glycation endproducts and their cellular receptor RAGE in diabetic nephropathy and non-diabetic renal disease. J Am Soc Nephrol 2000, 11:1656–1666
24. Hofmann MA, Drury S, Fu C, Qu W, Taguchi A, Lu Y, Avila C, Kambham N, Bierhaus A, Nawroth P, Neurath MF, Slattery T, Beach D, McClary J, Nagashima M, Morser J, Stern D, Schmidt AM: RAGE mediates a novel proinflammatory axis: a central cell surface receptor for S100/calgranulin polypeptides. Cell 1999, 97:889–901
25. Kislinger T, Fu C, Huber B, Qu W, Taguchi A, Yan SD, Hofmann M, Yan SF, Pischetsrieder M, Stern D, Schmidt AM: N^{ϵ} (carboxymethyl-)lysine modifications of proteins are ligands for RAGE that activate cell signalling pathways and modulate gene expression. J Biol Chem 1999, 274:31740–31749
26. Esposito C, Gerlach H, Brett J, Stern D, Vlassara H: Endothelial receptor-mediated binding of glucose-modified albumin is associated with increased monolayer permeability and modulation of cell surface coagulant properties. J Exp Med 1989, 170:1387–1407
27. Schmidt AM, Hasu M, Popov D, Zhang JH, Chen J, Yan SD, Brett J, Cao R, Kuwabara K, Costache G, Simionescu N, Simionescu M, Stern D: Receptor for advanced glycation endproducts (AGEs) has a central role in vessel wall interactions and gene activation in response to circulating AGE proteins. Proc Natl Acad Sci USA 1994, 91:8807–8811
28. Schmidt AM, Hori O, Chen J, Brett J, Stern D: AGE interaction with their endothelial receptor induce expression of VCAM-1: a potential mechanism for the accelerated vasculopathy of diabetes. J Clin Invest 1995, 96:1395–1403
29. Schmidt AM, Yan SD, Brett J, Mora R, Nowygrod R, Stern D: Regulation of mononuclear phagocyte migration by cell surface binding proteins for advanced glycosylation endproducts. J Clin Invest 1993, 92:2155–2168
30. Miyata T, Hori O, Zhang JH, Yan SD, Ferran L, Iida Y, Schmidt AM: The receptor for advanced glycation endproducts (RAGE) mediates the interaction of AGE-β_2-microglobulin with human mononuclear phagocytes via an oxidant-sensitive pathway: implications for the pathogenesis of dialysis-related amyloidosis. J Clin Invest 1996, 98: 1088–1094
31. Owen Jr WF, Hou FF, Stuart RO, Kay J, Boyce J, Chertow GM, Schmidt AM: β_2-Microglobulin modified with advanced glycation end products modulates collagen synthesis by human fibroblasts. Kidney Int 1998, 53:1365–1373
32. Marova I, Zahejsky J, Sehnalova H: Non-enzymatic glycation of epidermal proteins of the stratum corneum in diabetic patients. Acta Diabetol 1995, 32:38–43
33. Schleicher ED, Wagner E, Nerlich AG: Increased accumulation of the glycoxidation product N(epsilon)-(carboxymethyl)lysine in human tissues in diabetes and aging. J Clin Invest 1997, 99:457–468
34. Monnier VM, Bautista O, Kenny D, Sell DR, Fogarty J, Dahms W, Cleary PA, Lachin J, Genuth S: Skin collagen glycation, glycoxidation, and crosslinking are lower in subjects with long-term intensive versus conventional therapy of type 1 diabetes: relevance of glycated collagen products versus HbA1c as markers of diabetic complications. DCCT Skin Collagen Ancillary Study Group. Diabetes Control and Complications Trial. Diabetes 1999, 48:870–880
35. Coleman D: Diabetes—obesity syndromes in mice. Diabetes 1982, 31:1–6
36. Wyse B, Dulin W: The influence of age and dietary conditions on diabetes in the db mouse. Diabetologia 1970, 6:268–273
37. Wautier JL, Zoukourian C, Chappey O, Wautier MP, Guillausseau PJ, Cao R, Hori O, Stern D, Schmidt AM: Receptor-mediated endothelial cell dysfunction in diabetic vasculopathy: soluble receptor for advanced glycation endproducts blocks hyperpermeability. J Clin Invest 1996, 97:238–243
38. Mast BA, Schultz GS: Interactions of cytokines, growth factors, and proteases in acute and chronic wounds. Wound Rep Reg 1996, 4:411–420
39. Trengove NJ, Stacey MC, Macauley S, Bennett N, Gibson J, Burslem F, Murphy G, Schultz G: Analysis of the acute and chronic wound environments: the role of proteases and their inhibitors. Wound Rep Reg 1997, 7:442–452
40. Neely AN, Clendening CE, Gardner J, Greenhalgh DG: Gelatinase activities in wounds of healing-impaired mice versus wounds of nonhealing impaired mice. J Burn Care Rehabil 2000, 21:395–402
41. Chen C, Schultz GS, Bloch M, Edwards PD, Tebes S, Mast BA: Molecular and mechanistic validation of delayed healing rat wounds as a model for human chronic wounds. Wound Rep Reg 1997, 7:486–494
42. Brown DL, Kao WW, Greenhalgh DG: Apoptosis down-regulates inflammation under the advancing epithelial wound edge: delayed patterns in diabetes and improvement with topical growth factors. Surgery 1997, 121:372–380
43. Kane CD, Greenhalgh DG: Expression and localization of p53 and bcl-2 in healing wounds in diabetic and nondiabetic mice. Wound Rep Reg 2000, 8:45–58
44. Greenhalgh DG: The role of growth factors in wound healing. J Trauma 1996, 41:159–167
45. Wieman TJ: Clinical efficacy of becaplermin (rhPDGF-B) gel. Becaplermin Gel Studies Group. Am J Surg 1998, 176(Suppl 2a):74S–79S
46. Embil JM, Papp K, Sibbald G, Tousignant J, Smiell JM, Wong B, Lau CY: Recombinant human platelet-derived growth factor-B (becaplermin) for healing chronic lower extremity diabetic ulcers: an open-label clinical evaluation of efficacy. Wound Rep Reg 2000, 8:162–168